Int. J. of Applied Mechanics and Engineering, 2003, vol.8, No.1, pp.27-41

NONLINEAR VISCOELASTIC BEHAVIOR OF FLEXIBLE CELLULAR PLASTICS: REFINED ROD MODEL

D.A. CHERNOUS, S.V. SHILKO*,
D.A. KONYOK and Yu.M. PLESKACHEVSKY
V.A. Belyi Metal-Polymer Research Institute
Belarussian Academy of Sciences
32A Kirov Str., 246050 Gomel, BELARUS
e-mail: depa10@tut.by

A new technique of modelling nonlinear viscoelastic behavior of low-density flexible foams including cellular plastics used in advanced implants, namely, artificial analogs of periodont of the dental system and trabecular bones of the skeletal system has been developed. The material microstructure is modeled by a rod structure with chaotically oriented cubic cells. Young's modulus and critical strain (i.e., the case of stability loosing) dependence on the solid state phase fraction of flexible cellular plastics has been investigated. The dependences of tangential stress on shear strain, hydrostatic pressure on volume strain and axial stress on longitudinal deformation with taking into account solid phase viscosity at a given strain rate have been obtained for the simulated materials. The numerical results led to the conclusion that at a certain compression rate the transversal strain factor of a material becomes negative.

Key words: flexible foams, cellular structures, implants, large rod deflections, viscoelastic behavior, structural unit.

1. Introduction

Cellular plastics, including foams, are very efficient structures with respect to optimizing the strength and stiffness at preserved weight. Such materials are commonly employed in cushioning, insulating, damping, packing etc. Stiff foam is currently used in many load-bearing applications aimed at optimizing the strength to weight ratio of structural elements. Compliant foam is used in other applications, such as seat cushions and sponges.

The term cellular is appropriate when the material contains polyhedral closed cells, as if it had resulted from solidification of a liquid foam. Often they have no proper cells (Chan and Evans, 1997), although such materials are commonly classified as cellular. Recently, we have begun to realize the potential of these materials and as a result these cellular solids are increasingly used for structural applications, for insulation, for load bearing, for absorbing the kinetic energy from impact (Gibson and Ashby, 1998), as well as a lightweight core in sandwich panels. Encouraged by the engineering potential of cellular materials, one is motivated to understand the mechanical behavior of the cellular solid.

So, all the materials mentioned above may be useful for creating advanced soft implants, namely, the artificial analogs of periodont of the human dental system (Nyashin *et al.*, 1999) and trabecular bones of the skeletal system (Overaker *et al.*, 1999). But the mechanical properties of implant structures which imitate essentially the non-linear deformation behavior of their vital prototypes, i.e., biotissues, should be studied more thoroughly. Thus, to predict the deforming behaviour of such materials under various types of loading the corresponding mathematical models should be developed.

2. Simulation technique

For the open-cell flexible cellular plastics structure simulation we use a rod structural unit with chaotically oriented cubic cells (Warren and Kraynik, 1987; Dement'ev and Tarakanov, 1970a). We characterized the deformational behavior of the simulated material by the deforming process of the structural unit, presented in Fig.1.

* To whom correspondence should be addressed

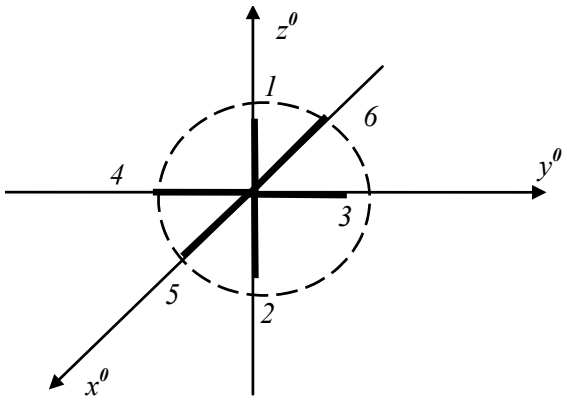

Fig.1. Structural unit of flexible cellular plastics.

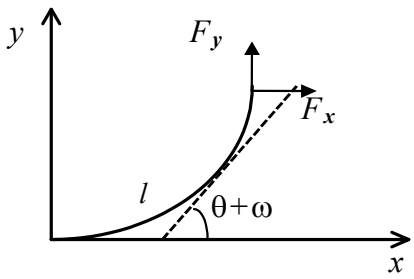

Fig.2. Scheme of cantilever beam under strong bending.

It is worth mentioning that such kind of a unit cell model with chaotically oriented cubic cells had already been simulated by Warren and Kraynik (1987). However, there had been used not a spherical, but a cubic structural unit. Besides, the shear deformation of rods also had not been taken into account there.

Structural unit rods in Fig.1 are directed normally to cubic planes. Symmetry of the element allows one to represent the displacement of force application points (ends of rods) relatively to the rods joints through the deformation tensor components.

$$\Delta x_{L1} = x_{L1} - L = L\varepsilon_{z^0 z^0}, \quad y_{L1} = \frac{L}{2}\sqrt{\gamma_{x^0 z^0}{}^2 + \gamma_{y^0 z^0}{}^2},$$

$$\Delta x_{L3} = x_{L3} - L = L\varepsilon_{y^0 y^0}, \quad y_{L3} = \frac{L}{2}\sqrt{\gamma_{x^0 y^0}{}^2 + \gamma_{y^0 z^0}{}^2}, \tag{2.1}$$

$$\Delta x_{L5} = x_{L5} - L = L\varepsilon_{x^0 x^0}, \quad y_{L5} = \frac{L}{2}\sqrt{\gamma_{x^0 y^0}{}^2 + \gamma_{x^0 z^0}{}^2}$$

where L – the structural unit rod length; x_{Li}, y_{Li} – coordinates for the end of the i-th rod $(i = 1...6)$ in the xy coordinate system; the x axis is directed longitudinally to the i-th rod in a non-deformed state (Fig.2).

Equation (2.1) refers to the deformations for which the Cauchy relations are satisfied (Landau *et al*., 1986). Here the value of parameter L can be related to the solid state volumetric fraction by the following equation

$$V_f = \frac{V_m}{V} = \frac{9}{2\pi q^2} \tag{2.2}$$

where V_m – the volume of rods in a structural unit; V – the structural unit total volume before deformation; q – the rod length L to its cross sectional side length r ratio. For simplification we neglected the volume of the node (rod joints) and assumed that rods are of a square cross-section. During further calculations we have estimated that results of modeling do not depend on the r value. So we may assume that $r = 1, L = q$.

Let us assume that in the coordinate system $X\,Y\,Z$ the uniaxial strain is defined as $\varepsilon_{nm} = f(t)$ (other components of strain are equal to zero). The system $X\,Y\,Z$ position related to starting $x^0\,y^0\,z^0$ one is defined by Euler's angles $\beta_1, \beta_2, \beta_3$. Once the function $f(t)$ and Euler's angles are known, let us define deformation components in the $x^0\,y^0\,z^0$ system (Fig.1). Then, displacements Eq.(2.1) can be written as follows

$$y_{Li} = \varepsilon_{nm}(t)\eta_i(\beta_1,\beta_2,\beta_3), \quad \Delta x_{Li} = \varepsilon_{nm}(t)\xi_i(\beta_1,\beta_2,\beta_3). \tag{2.3}$$

Here $\eta_i(\beta_1,\beta_2,\beta_3), \xi_i(\beta_1,\beta_2,\beta_3)$ – Euler's angle functions which are related to the recalculation of tensor components at coordinate axis rotation (Starovoitov, 2001). For the determination of forces $\boldsymbol{F}_i$ acting at the ends of rods by the set deflections it is necessary to solve a strong flexure problem of a cantilever beam taking into account material viscosity. At the same time, to describe the deformation of the low-density porous materials $(V_f < 0.1)$ it can be assumed that the rod is deformed equally at all its length *L*. Viscoelastic behavior of the rod material is described by Rzhanitsyn's relaxation kernel (Rzhanitsyn, 1968)

$$R(t) = Ae^{-\beta t}t^{\alpha-1} \tag{2.4}$$

where *t* – time, *s*; *A*, α, β – kernel parameters.

Stress to strain relations are determined by the following equation (Starovoitov, 2001)

$$s_{\rho\chi} = 2G_f\left(\upsilon_{\rho\chi} - \int_0^t R(t-\tau)\upsilon_{\rho\chi}(\tau)d\tau\right), \quad \sigma = 3K_f\varepsilon \tag{2.5}$$

where $s_{\rho\chi}, \upsilon_{\rho\chi}, \sigma, \varepsilon$ – the deviator and spherical parts of stress and strain tensors; G_f, K_f – shear and bulk modules of the material, correspondingly.

For the beam deformations let us assume

$$\varepsilon_{ll} = \varepsilon_0(l) + \lambda\theta'(l), \quad \varepsilon_{\lambda l} = \frac{1}{2}\omega(l) \tag{2.6}$$

where *l* – the coordinate along the rod median in the deformed state; λ – the coordinate perpendicular to *l*; θ – the turning angle of the rod cross-section connected with flexural strain; $\theta' - \theta$ derivative of *l* coordinate; ω – the rod cross-section turning angle as a function of shear strain; ε_0 – the deformation of a center line passing through the cross section gravity center under tension or compression.

Allowance for flexural, shear and tensile-compression strains helps to describe the deformation of "short" rods when their length is commensurable with the cross-section side length. For an arbitrary cross-section shape the following expressions are valid

$$M = \iint_S \sigma_{ll}\lambda dS, \quad P = \iint_S \sigma_{ll}dS, \quad Q = \iint_S \sigma_{\lambda l}dS \tag{2.7}$$

where *M* – the bending moment; *Q*, *P* – the transverse and longitudinal forces. So, equilibrium equations for the cantilevered rod for the large deflections case will take the form

$$\begin{gathered} Q = F_y\cos(\theta+\omega) - F_x\sin(\theta+\omega), \quad P = F_x\cos(\theta+\omega) + F_y\sin(\theta+\omega), \\ M = F_y(x_L - x) - F_x(y_L - y). \end{gathered} \tag{2.8}$$

Substituting Eqs.(2.5) and (2.6) into (2.7) gives

$$\omega = \frac{-k}{G_f S}\left(F_x\sin(\theta+\omega) - F_y\cos(\theta+\omega)\right) + \int_0^t R(t-\tau)\omega(\tau)d\tau, \tag{2.9}$$

$$\varepsilon_0 = \frac{1}{E_f S}\left(F_y \sin(\theta+\omega) + F_x \cos(\theta+\omega)\right) + \int_0^t R(t-\tau)\varepsilon_0(\tau)d\tau,$$

$$\theta' = \frac{1}{E_f J}\left(F_y\left(L+\varepsilon_{nm}\xi - x\right) - F_x\left(\varepsilon_{nm}\eta - y\right)\right) + \int_0^t R(t-\tau)\theta'(\tau)d\tau, \qquad \text{cont.(2.9)}$$

$$x' = \cos(\theta+\omega), \quad y' = \sin(\theta+\omega)$$

where J, S – the moments of inertia and cross-section area of the rod, correspondingly; E_f – Young's modulus of the rod material; k – the coefficient complying with non-uniformity of tangential stress distribution over the cross-section area. At our calculations we assumed $k = 1$.

So a system of equations was obtained for the five unknown coordinates l and time functions. Let us initialize the following boundary conditions: $\theta(0,t) = x(0,t) = y(0,t) = 0$. In Eq.(2.9) η, ξ are constants. A solution to these combined equations using finite difference method make it possible to obtain free end of rod coordinates as a function of five variables

$$x_L = x(L,t) = f_x(F_x, F_y, \eta, \xi, t), \quad y_L = y(L,t) = f_y(F_x, F_y, \eta, \xi, t). \qquad (2.10)$$

During computation of Eqs.(2.9) it was taken into account that l coordinate differentiation is made in deformed state. So, an increment of l parameter was assumed equal to $dl = (l+\varepsilon_0)\frac{L}{n_0}$. Here, n_0 is a discretization number. Equation (2.9) was solved for the set t. It should be mentioned that the structure of Rzhanitsyn's relaxation kernel Eq.(2.4) causes that integral items in Eq.(2.9) contain θ, γ and ε_0 functions which were defined during the previous steps.

The conditions for the calculation of the sought forces is of the type

$$\begin{cases} f_x(F_x, F_y, \eta, \xi, t) = L + \varepsilon_{nm}(t)\xi, \\ f_y(F_x, F_y, \eta, \xi, t) = \varepsilon_{nm}(t)\eta. \end{cases} \qquad (2.11)$$

Equations (2.9) and (2.11) were solved with the help of MathCad® 7.0 software. The system of nonlinear equations was solved using Newton's method (Hudson, 1964). As the initial approximation we took the solution of the previous step. So we obtain $F_x(\eta, \xi, t)$, $F_y(\eta, \xi, t)$ functions which can be presented as follows

$$F_x = C_{x1}\xi + C_{x2}\eta + C_{x3}\xi\eta + C_{x4}\xi^2 + C_{x5}\eta^2 + C_{x6}\xi^2\eta + C_{x7}\xi\eta^2 + C_{x8}\xi^3 + C_{x9}\eta^3 + C_{x10}\xi^2\eta^2. \quad (2.12)$$

At given t, coefficients $C_{xj}, C_{yj}\,(j = 1...10)$ can be defined by the standard regression procedures (Hudson, 1964). Stress tensor components are related through forces Eq.(2.12) as follows

$$\sigma_{x^0x^0} = F_{x1}\frac{1}{\pi(L+\varepsilon_{nm}\xi_2)(L+\varepsilon_{nm}\xi_3)}, \quad \sigma_{y^0y^0} = F_{x2}\frac{1}{\pi(L+\varepsilon_{nm}\xi_1)(L+\varepsilon_{nm}\xi_3)},$$

$$\sigma_{z^0z^0} = F_{x3}\frac{1}{\pi(L+\varepsilon_{nm}\xi_1)(L+\varepsilon_{nm}\xi_2)}, \qquad (2.13)$$

$$\sigma_{x^0y^0} = F_{y1}\frac{1}{\pi\left(L+\varepsilon_{nm}\xi_2\right)\left(L+\varepsilon_{nm}\xi_3\right)}\frac{\varepsilon_{x^0y^0}}{\left(\varepsilon_{x^0y^0}{}^2+\varepsilon_{x^0z^0}{}^2\right)^{1/2}},$$

$$\sigma_{x^0z^0} = F_{y1}\frac{1}{\pi\left(L+\varepsilon_{nm}\xi_2\right)\left(L+\varepsilon_{nm}\xi_3\right)}\frac{\varepsilon_{x^0z^0}}{\left(\varepsilon_{x^0y^0}{}^2+\varepsilon_{x^0z^0}{}^2\right)^{1/2}}, \qquad \text{cont.(2.13)}$$

$$\sigma_{y^0z^0} = F_{y2}\frac{1}{\pi\left(L+\varepsilon_{nm}\xi_1\right)\left(L+\varepsilon_{nm}\xi_3\right)}\frac{\varepsilon_{y^0z^0}}{\left(\varepsilon_{x^0y^0}{}^2+\varepsilon_{y^0z^0}{}^2\right)^{1/2}}.$$

Then stresses for *X Y Z* system were redefined. Because of the chaotic orientation of the unit cells of the model obtained stress tensor components should be averaged by direction (Euler's angles)

$$\sigma_{nm} = \int_0^{\pi}\int_0^{2\pi}\int_0^{2\pi}\sigma_{nm}\left(\beta_1,\beta_2,\beta_3\right)\frac{\sin\beta_3}{8\pi^2}d\beta_1 d\beta_2 d\beta_3. \qquad (2.14)$$

So, for the known stress to time dependence we defined time dependencies of stresses in a representative volume of the material.

3. Calculation examples

3.1. Shear strain

As an example of realizing the above technique let us examine the stress-strain state of an elastic porous material based on the high density polyethylene (HDPE). Viscoelastic characteristics of this material can be obtained by experimental data processing. Experimental data for HDPE were obtained by Goldman (1979): $G_f = 237\,MPa$, $K_f = 1402\,MPa$, $A = 0.022\,s^{-\beta}$, $\beta = 2.995\cdot 10^{-5}\,s^{-1}$, $\alpha = 0.175$. We examined the pure shear strain $\gamma(t) = 0.05t$. Here, $\gamma = \gamma_{XZ} = 2\varepsilon_{XZ}$ (all other deformation components are accepted equal to zero). After redefinition of tensor components and homogenization operations Eq.(2.14) we obtained the following expression for the tangential strain $\sigma_{XZ} = \tau$

$$\begin{aligned}\tau\cdot 10^{-3} = &\left(50\frac{1}{L}C_{x1} + 12C_{x3} + 3.5LC_{x7} + 7.1LC_{x8} + 75\frac{1}{L}C_{y2} + 12C_{y4} + \right.\\ &+ 28C_{y5} + 3.6LC_{y6} + 11LC_{y9} + 1.1L^2C_{y10}\left.\right) + \gamma\left(12\frac{1}{L}C_{x2} + 7.1C_{x4} + 3.6C_{x5} + \right.\\ &\left.+ 1.5LC_{x6} + 1.1LC_{x9} + 0.4L^2C_{x10} + 12\frac{1}{L}C_{y1} + 3.6C_{y3} + 1.1LC_{y7} + 1.5LC_{y8}\right).\end{aligned} \qquad (3.1)$$

Assuming that the volume of the structural unit does not change, the following equation is satisfied

$$\left(L+\Delta x_{L1}\right)\left(L+\Delta x_{L2}\right)\left(L+\Delta x_{L3}\right) = L^3. \qquad (3.2)$$

The dependence of $\tau(\gamma_{XZ})$ for simulated materials are presented in Fig.3 at $V_f = 0.01$ (Fig.3a), $V_f = 0.02$ (Fig.3b) and at $V_f = 0.04$ (Fig.3c). The diagram in Fig.3a and the curve *1* in Fig.3b,c were plotted taking into the solid phase viscosity and the curve *2* – with it. Dotted line corresponds to linear dependence $\tau(\gamma)$.

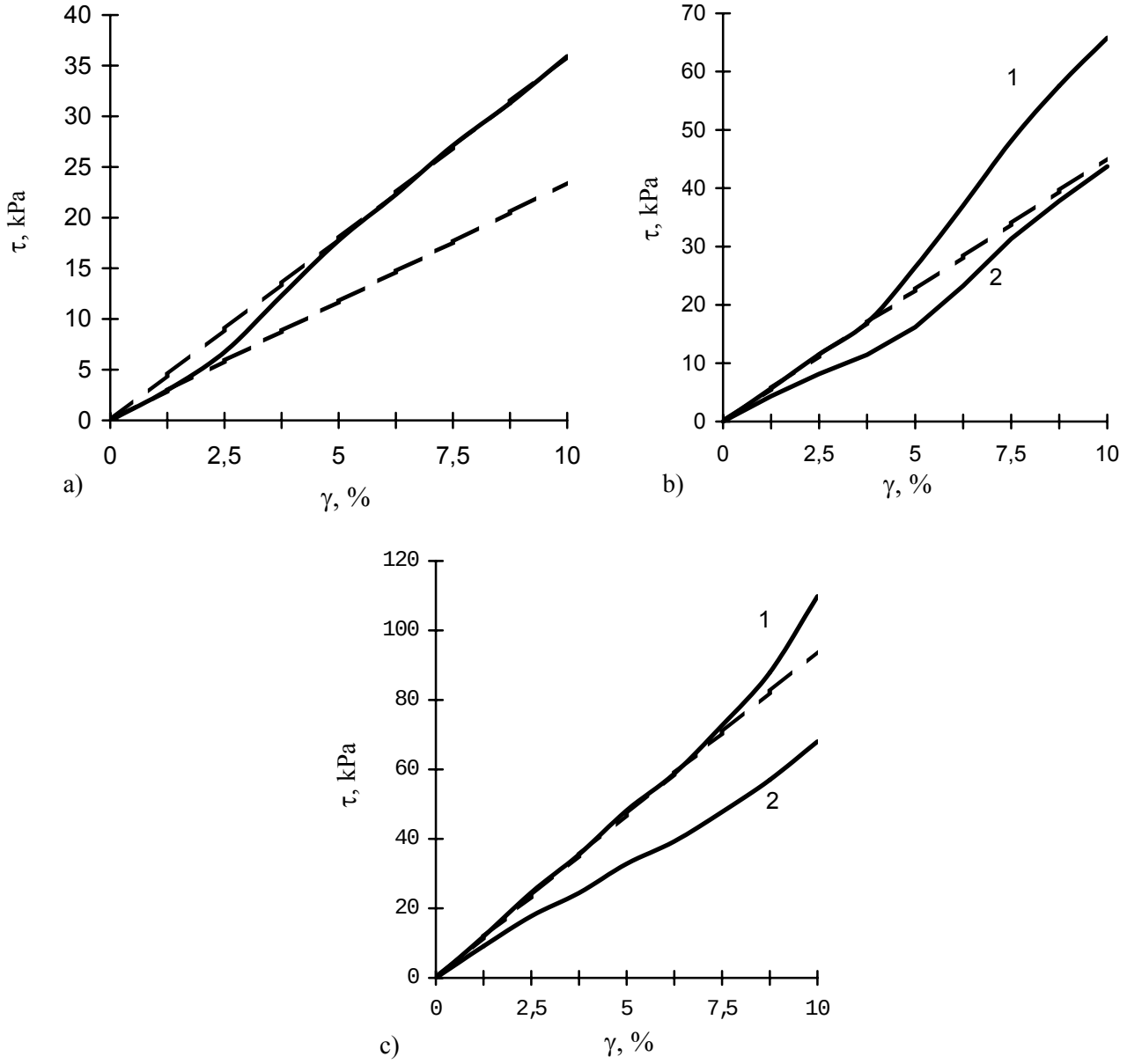

Fig.3. Dependence of shear stress on shear strain for the flexible cellular plastics at $V_f = 0.01\,(a)$, $0.02\,(b)$ and $0.04\,(c)$.

Based on the analysis of the dependences obtained we have come to the following conclusions:

- Linear elasticity equations $\tau = G\gamma$ are true at low shear angles $\gamma < 0.025$. Initial shear resistance of the material decreases with the strain rate drop.
- As shear strain reaches some critical value γ_{cr} the material stiffness evenly increases. At strain rate decreasing the effect of the increasing shear stiffness smoothes. The value of γ_{cr} is independent of the strain rate and increases as V_f rises.

- At high shear strains $(\gamma > 3\gamma_{cr})\,\tau(\gamma)$ the dependence becomes linear again: $\tau = G^0\gamma$ and $G^0 > G$.

These peculiarities agree with experimental results on elastic polyurethane foam deformation published elsewhere (Hilyard and Cunningham, 1994). A more detailed quantitative comparison is problematic due to lack of experimental data on the shear strain of elastic cellular plastics.

3.2. Volume strain

For the examination of strain behavior of porous materials at a uniform compression (tension) the given volume strain $\Theta = \Delta V/V$ defines Δx_L shear which is identical for all the rods of spherical structural unit $\Delta L = L\left[(\Theta+1)^{1/3} - 1\right]$. So the system of Eqs.(2.9) will be simplified

$$\omega = \frac{-k}{G_f S}F_x\sin(\theta+\omega) + \int_0^t R(t-\tau)\omega(\tau)\,d\tau, \qquad \varepsilon_0 = \frac{1}{E_f S}F_x\cos(\theta+\omega) + \int_0^t R(t-\tau)\,\varepsilon_0(\tau)\,d\tau,$$
$$\theta' = \frac{-F_x(y_L - y)}{E_f J} + \int_0^t R(t-\tau)\,\theta'(\tau)\,d\tau, \quad x' = \cos(\theta+\omega), \quad y' = \sin(\theta+\omega). \tag{3.3}$$

Equations (2.11) will transform into

$$\begin{cases} f_x(F_x, y_L, t) = L + \Delta x_L, \\ \\ f_y(F_x, y_L, t) = y_L. \end{cases} \tag{3.4}$$

Solution of these combined Eqs.(3.4) allows one to define functions $F_x(\Delta x_L, t),\, y_L(\Delta x_L, t)$. Hydrostatic pressure is conditioned in deformed state by the force F_x as follows

$$p = \frac{3F_x}{2\pi(L+\Delta x_L)^2}. \tag{3.5}$$

So, at a given volume strain we can define the time dependence of hydrostatic pressure $p(t)$.

Dependences of $p(\Theta)$ obtained for HDPE at $V_f = 0.01$ are presented in Fig.4. Volume strain $\Theta(t)$ changes in time under the law $\Theta(t) = -0.08t$. The curves *1* and *3* in Fig.4 were plotted neglecting solid phase viscosity; the curve *1* presents hydrostatic pressure Eq.(3.5) dependence on volume strain; the curve *3* corresponds to stress defined as: $p = \frac{3F_x}{2\pi L^2}$. The curve *2* in Fig.4 was plotted with allowance for solid phase viscosity.

At simulation of elastic behavior of a material with a small volumetric portion of solid phase $q >> 1$ we used the simplified expression for the force F_x

$$F_x = \begin{cases} -E_f J\left(p_0 - \dfrac{4\Delta x_L}{LC_1^{\,2}}\right) & \text{if} \quad E_f S\dfrac{\Delta x_L}{L} < -\pi^2\dfrac{E_f J}{4L^2}, \\ \\ E_f S\dfrac{\Delta x_L}{L} & \text{if} \quad E_f S\dfrac{\Delta x_L}{L} \ge -\pi^2\dfrac{E_f J}{4L^2}, \end{cases} \tag{3.6}$$

obtained by the small parameter method (Gromov and Raetzki, 1971). Here $p_0 = \frac{\pi^2}{4L^2}$, $C_1 = \frac{2\sqrt{2}}{\sqrt{p_0}}$. During a supercritical rod behavior only the rod flexure was taken into account in the latter expression. Results obtained by Eqs.(3.6) for $V_f = 0.01$ practically coincided with the curve *1* in Fig.4. Analysis of Fig.4 leads to the following conclusion:

- At low volume strains $(\Theta < 0.0005)$ $\sigma(\Theta)$ curve is practically linear. As the strain rate decreases the bulk modulus of the material decreases too.
- When the volume strain reaches some critical point Θ_{cr}, the stiffness of the porous material reduces stepwise. This can be explained by the fact that the unit cell ribs lose stability. So, Eqs.(3.6) for Θ_{cr} yields

$$\Theta_{cr} \approx \frac{\pi^3}{72} V_f . \tag{3.7}$$

Critical volume strain values do not depend on the strain rate.

- A further increase of hydrostatic pressure is caused mainly by a reduction of the surface area of the compressed material. At the same time, the force F_x which affects the cell ribs does not practically increase.

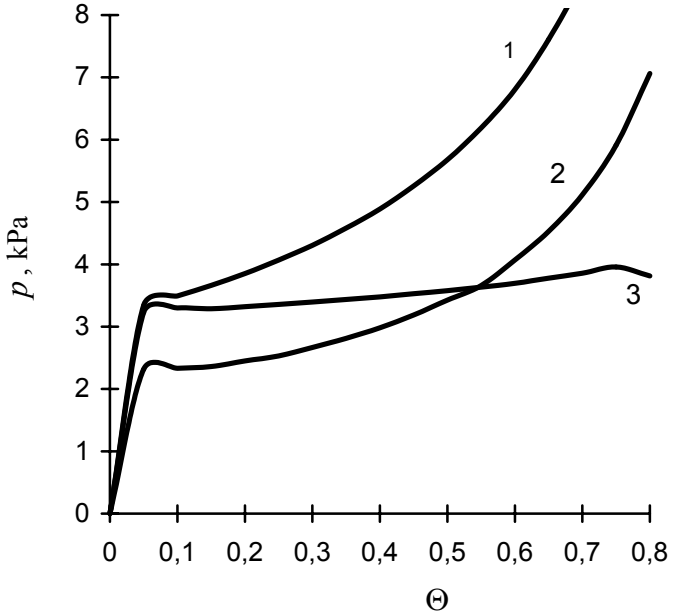

Fig.4. Dependence of hydrostatic pressure *p* on volume strain for cellular plastics.

3.3. Uniaxial stress

Averaging in all possible loading directions Eq.(2.14) makes the simulated material isotropic at a macroscopic level. So the $\tau(\gamma)$ function characterizes the dependence of stress on strain deviators components $\tau(\gamma) = s_{nm}(2\upsilon_{nm})$. Thus if the functions $\tau(\gamma)$ and $p(\Theta)$ are known, it is possible to simulate isotropic material behaviour at an arbitrary homogeneous stress-strain state. Hence, for the uniaxial stress $(\sigma_{ZZ} \neq 0)$ the following relations are true

$$2\upsilon_{ZZ} = \frac{4}{3}\varepsilon_{ZZ}(1+\mu), \quad \Theta = (1+\varepsilon_{ZZ})(1-\varepsilon_{ZZ}\mu)^2 - 1, \qquad s_{ZZ} = \frac{2}{3}\sigma_{ZZ}, \quad \sigma = \frac{1}{3}\sigma_{ZZ} . \tag{3.8}$$

We introduce the transversal strain factor $\mu = -\frac{\varepsilon_{XX}}{\varepsilon_{ZZ}}$, which is analogous to Poisson's ratio in the linear elasticity region. Making all allowance for strong bending flexures of ribs where μ depends on the strain ε_{ZZ}, the dependence is determined by the following equation

$$\tau\left(\frac{4}{3}\varepsilon_{ZZ}(1+\mu)\right) = 2p\left((1+\varepsilon_{ZZ})(1-\varepsilon_{ZZ}\mu)^2 - 1\right). \tag{3.9}$$

It was obtained that the $\mu(\varepsilon_{ZZ})$ function does not depend on the strain rate. In Fig.5 the dependence of the transverse deformation factor μ on the longitudinal strain ε_{ZZ} at stretching (a) and compression (b) of an elastic cellular plastic based on HDPE $(V_f = 0.01)$ is presented. Upon compression the strain reaches some critical value ε_{ZZ}, μ rapidly decreases and becomes negative at $\varepsilon_{ZZ} > 0.9\%$. Such an abnormality of elastic behavior was experimentally observed in polyurethane (Choi and Lakes, 1995; Chan and Evans, 1997) and polyethylene (Brandel and Lakes, 2001) foams. Earlier investigations showed that this effect may occur in cellular materials with a honeycomb microstructure (Shilko *et al*., 1998) or a tetrakaidecahedral cell when the cell ribs are buckled inward (Choi and Lakes, 1995).

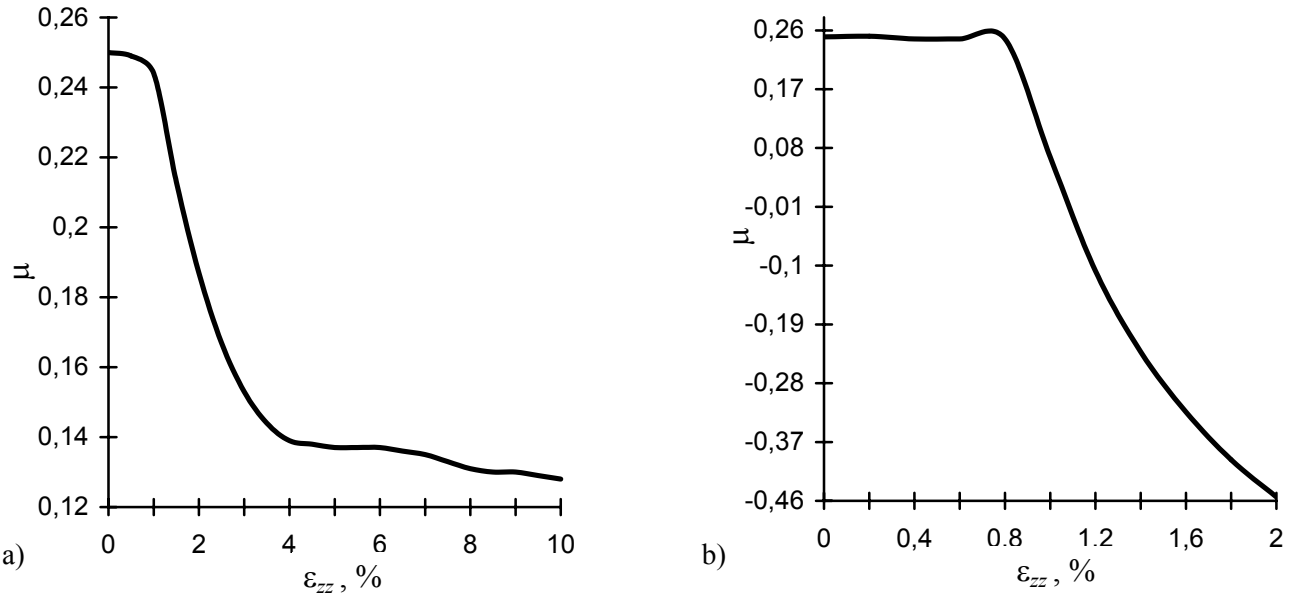

Fig.5. Dependence of transversal strain factor μ on longitudinal strain ε_{ZZ} at stretching (a) and compression (b) of flexible cellular plastics.

At stretching μ also decreases rapidly while the strain reaches ε_{cr}. Besides, the $\mu(\varepsilon_{ZZ})$ dependence rapidly passes on the horizontal plateau $\mu(\varepsilon_{ZZ}) = const = \nu^0$, where ν^0 is defined as

$$\nu^0 = \frac{3K - 2G^0}{6K + 2G^0} \tag{3.10}$$

here K – the foam bulk modulus defined by the initial part of the $p(\Theta)$ curve; G^0 – the shear modulus defined by the $\tau(\gamma)$ curve.

This enabled us to make the following conclusions:

- At small strains the μ value remains constant and coincides with Poisson's ratio.
- Upon compression the strain reaches some critical value ε_{cr}, μ rapidly decreases and becomes negative at $\varepsilon_{ZZ} > 0.9\%$.
- At stretching μ decreases rapidly while the strain reaches ε_{cr} and $\mu(\varepsilon_{ZZ})$ dependence rapidly passes on the horizontal plateau.

By defining the $\mu(\varepsilon_{ZZ})$ function the dependence of stress σ_{ZZ} on strain ε_{ZZ} can be obtained

$$\sigma_{ZZ}(\varepsilon_{ZZ}) = \frac{3}{2}\tau\left(\frac{4}{3}\varepsilon_{ZZ}\left[1+\mu(\varepsilon_{ZZ})\right]\right). \tag{3.11}$$

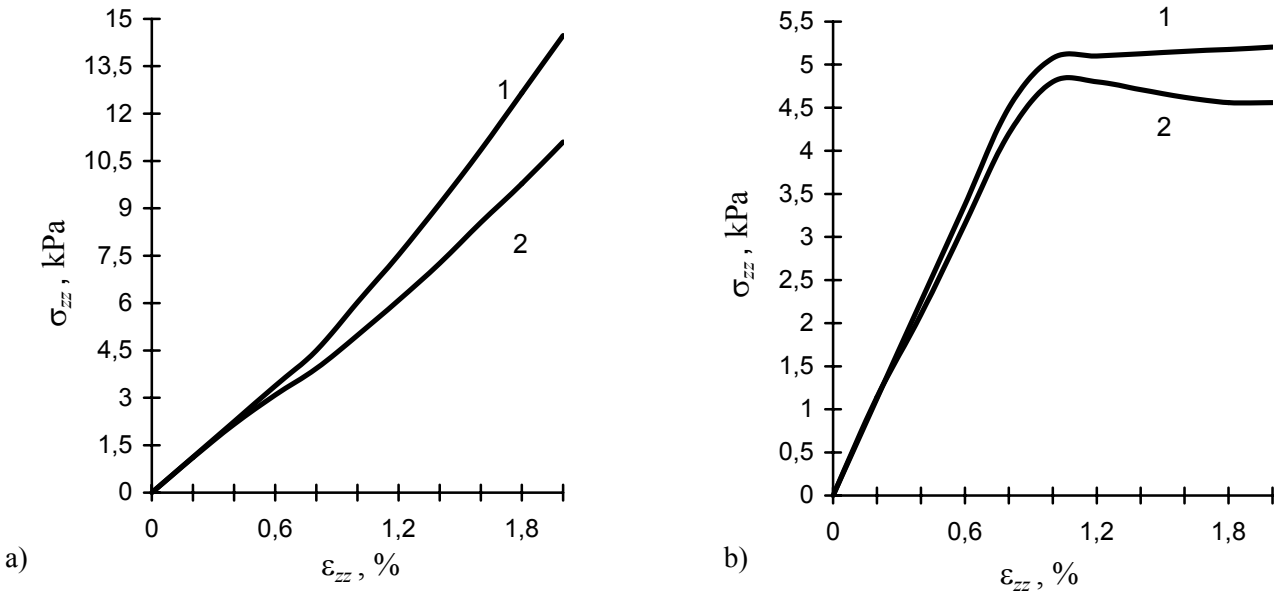

Fig.6. Dependence of stress σ_{ZZ} on longitudinal strain ε_{ZZ} at stretching (a) and compression (b) of flexible cellular plastics.

Stress on strain relations for the simulated foam described above $(V_f = 0.01)$ are presented in Fig.6. Curve *1* is plotted without taking account of the solid material viscosity $(A = 0)$ and the curve *2* corresponds to $0.1 s^{-1}(A \neq 0)$ strain rate. At a uniaxial stress the following peculiarities of $\sigma_{ZZ}(\varepsilon_{ZZ})$ relationship can be mentioned

- At small strains $\sigma_{ZZ}(\varepsilon_{ZZ})$ relationship is practically linear. Young's moduli *E* at compression and tension coincide and *E* values drop as the strain rate decreases.
- As soon as the compressive strain reaches the critical meaning ε_{cr} material stiffness decreases stepwise and henceforth the curve $\sigma_{ZZ}(\varepsilon_{ZZ})$ passes on the practically horizontal plateau. This is a characteristic feature of most flexible polymer foams (Weaire and Fortes, 1994; Choi and Lakes, 1995). ε_{cr} value does not depend on the strain rate.
- As the tensile strain reaches ε_{cr} the material gets toughened. This fact was confirmed in a number of experiments (Hilyard and Cunningham, 1994, Wang and Cuitiňo, 2000).

At small strains the stability of μ allows us to determine the correlation between $\varepsilon_{cr}, \Theta_{cr}, \gamma_{cr}$

$$\varepsilon_{cr} = \frac{1}{1-2\nu}\Theta_{cr}, \quad \gamma_{cr} = \frac{4(1+\nu)}{3(1-2\nu)}\Theta_{cr}. \tag{3.12}$$

4. Comparison with experimental data

To estimate the applicability of the theoretical model for foam deformation, the properties observed in experiments we compared with the calculated and experimental values of the relative Young's modulus E/E_f and critical strains ε_{cr} proceeding from the following considerations: The majority of experimental data on elastic foams deformation refer to their uniaxial compression; the calculated stress on strain dependence (Fig.6) as well as experimental one are almost linear at $\varepsilon < \varepsilon_{cr}$. As it was shown by Hilyard and Cunningham (1994), $\sigma_{ZZ}(\varepsilon_{ZZ})$ dependence at $\varepsilon_{ZZ} > \varepsilon_{cr}$ to a certain degree is conditioned by inhomogeneity of the material inner structure.

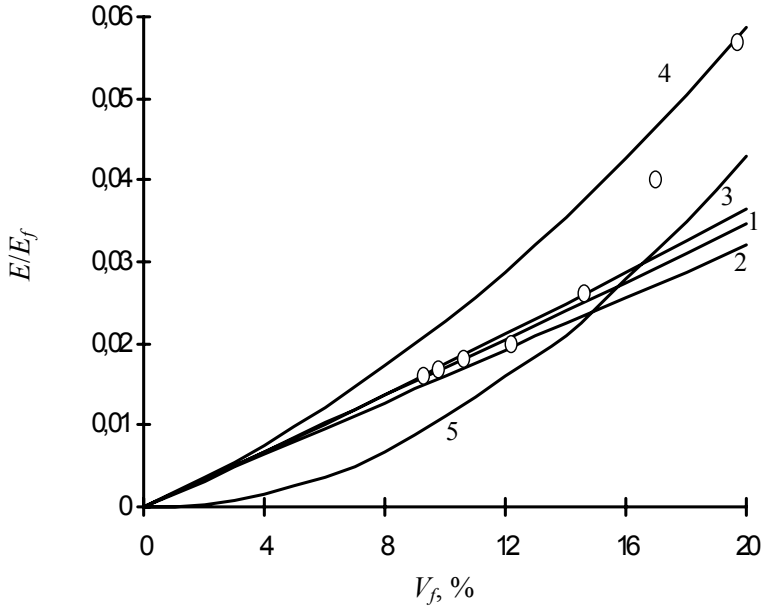

Fig.7. Dependence of relative Young's modulus E/E_f on the solid phase volumetric fraction V_f for the flexible foam.

While defining Young's modulus *E* of elastic cellular plastic we assumed that rod cross-section turning angles are small $(\cos(\theta+\omega)\approx 1, \sin(\theta+\omega)\approx 0)$ and did not consider rod viscosity. In this case solutions to Eqs.(2.9) and (2.11) can be obtained in an analytical form. For the relative Young's modulus we have

$$\frac{E}{E_f} = V_f \frac{36 + V_f\pi(7 + 4\nu_f)}{216 + 3V_f\pi(9 + 8\nu_f)} \tag{4.1}$$

where ν_f – the solid phase Poisson's ratio. In particular, for the elastic polymer material we assume $\nu_f = 0.49$. Expressions (3.7) and (3.12) also allow an approximate analytical expression for the critical strain ε_{cr}

$$\varepsilon_{cr} = \frac{V_f\pi^3\left[72 + V_f\pi(9 + 8\nu_f)\right]}{72\left[36 + V_f\pi(7 + 4\nu_f)\right]}. \tag{4.2}$$

The dependence of the relative Young's modulus E/E_f on the relative solid volume fraction V_f for the elastic foam is presented in Fig.7. In Fig.7 curve *1* corresponds to Eqs.(4.1). Line *2* in Fig.7 agrees with

the results obtained by Warren and Kraynik (1987). Line *3* meets the results obtained by Beverte and Kregers (1987) using the semi-axes hypothesis. Line *4* corresponds to the analytical expression

$$\frac{E}{E_f} = \frac{V_f}{3}\left(1 - 2\nu'\right) = 0.16V_f , \tag{4.3}$$

obtained by Gibson and Ashby (1982). Where ν' – Poisson's ratio of the material dependent on the number of rods in a structural unit *N*. For the simulation of mechanical behavior of rubber foam Gibson and Ashby (1982) used a structural element with $4 < N < 8$, when $\nu' = 0.26$. Curve *5* in Fig.7 corresponds to the empirical relation for the relative Young's modulus of foam rubbers (Hilyard and Cunningham, 1994)

$$\frac{E}{E_f} = \frac{V_f}{12}\left(2 + 7V_f + 3{V_f}^2\right). \tag{4.4}$$

Circles in Fig.7 reflect experimental data for the foam rubber (Hilyard and Cunningham, 1994; Dement'ev and Tarakanov 1970a; Lederman, 1971). Figure 7 proves that our technique makes it possible to predict quite accurately the stiffness of the simulated material at $V_f < 0.15$. At low V_f Young's modulus assumed by our simulation is identical to that Warren and Kraynik (1987). At high values of V_f Eq.(4.4) should be used. Certain errors arising at the application of the theory to materials with $V_f > 0.15$ are because at great V_f values, approximation of the rods used in our work becomes unacceptable.

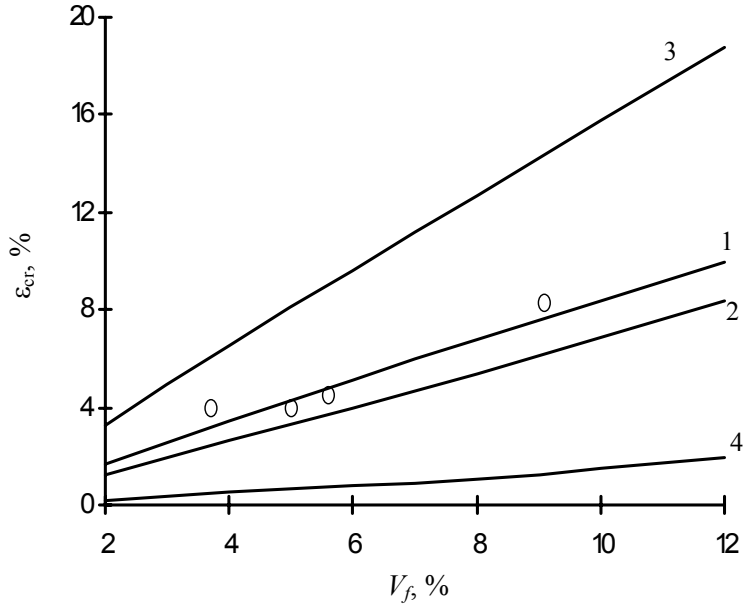

Fig.8. Dependence of critical strain ε_{cr} at uniaxial stress on solid phase volumetric fraction V_f.

In Fig.8 the dependence of critical strain ε_{cr} which corresponds to decreasing of material stiffness on the solid phase volume fraction V_f, is presented. Line *1* in Fig.8 was drawn using data obtained from Eq.(4.2). Line *2* is plotted in accordance with the technique proposed by Dement'ev and Tarakanov (1970b), which is based on the rod model analysis. The model consists of the ordered 14-faced cells. Dement'ev and Tarakanov (1970b) assumed that at compression the cell ribs experience only compressive load. Line *3* in Fig.8 is based on the results of cubic structural unit simulation proposed by Warren and Kraynik (1987). Line

4 in Fig.8 is built using equations obtained by Beverte and Kregers (1987). Circles in Fig.8 correspond to experimental values of ε_{cr} for elastic polyurethane, semirigid poly(vinyl chloride) and rubber foams (Hilyard and Cunningham,1994; Dement'ev and Tarakanov, 1970a). It is worth noting that our technique renders it possible to simulate mechanical behaviour of flexible foams and to predict ε_{cr} values more correctly as compared to other ones (Warren and Kraynik, 1987; Dement'ev and Tarakanov, 1970a,b; Weaire and Fortes, 1994).

5. Conclusions

The proposed model predicts the following features of experimental stress-strain curves for elastic cellular plastics:

1. Existence of critical strain. Its surpassing at compression gives rise to a sharp reduction in the material stiffness, while at stretching to its increase.
2. Young's modulus of a porous material decreases as the deformation rate decreases and the critical strain does not depend on the strain rate.

The technique ensures more accurate results in prediction of critical strain and Young's modulus values for the low-density $(V_f < 0.15)$ foams in contrast to these published elsewhere and may be employed in biomechanical design of human implants as well as in engineering (cushioning, insulating, damping, packing).

Acknowledgment

This work was supported by the grants of Belarussian and Russian fundamental research foundations (projects T02R-014 and T00M-020).

Nomenclature

C_{xj}, C_{yj} – expansion factors of force F_i components by Euler's angle function $(j = 1..10)$
F_i – force acting on the *i*-th rod end;
G, G^0 – shear modulus of porous material at small and large shear strains
G_f, K_f, E_f, ν_f – shear modulus, bulk modulus, Young's modulus and Poisson's ratio of rod material
J, S – inertial moment and cross-section area of the rod
k – coefficient denoting distribution inhomogeneity of tangential stress over cross-section area
L, r – common length and cross-sectional plane length of rod in structural unit
l – coordinate along rod median in deformed state
M – bending moment
p – hydrostatic pressure
$s_{\rho\chi}, \upsilon_{\rho\chi}, \sigma, \varepsilon$ – deviator and spherical parts of stress and strain tensors
Q, P – transverse and longitudinal forces
q – rod length to cross-section face length ratio
V_f – solid phase volume fraction
X, Y, Z – new coordinate system turned by $\beta_1, \beta_2, \beta_3$ angles relative to x^0, y^0, z^0
x, y – rod coordinate system
x^0, y^0, z^0 – basic Cartesian coordinate system for structural unit
x_{Li}, y_{Li} – *i*-th rod end coordinates
A, α, β – Rzhanitsyn's relaxation kernel parameters
$\beta_1, \beta_2, \beta_3$ – Euler's angles
γ – shear strain

$\gamma_{n^0m^0}$ – shear strains $\left(\gamma_{n^0m^0} = 2\varepsilon_{n^0m^0} \quad \text{at} \quad n^0 \neq m^0\right)$

ε_0 – strain of median passing gravity center of cross-section (tension-compression)

$\varepsilon_{n^0m^0}, \sigma_{n^0m^0}$ – stress and strain tensor components affecting structural unit in $x^0y^0z^0\left(n^0, m^0 = x^0, y^0, z^0\right)$ system

$\varepsilon_{nm}, \sigma_{nm}$ – stress and strain tensor components affecting structural unit in $XYZ(n, m = X, Y, Z)$ coordinate system

$\varepsilon_{cr}, \Theta_{cr}, \gamma_{cr}$ – critical longitudinal, volume and shear strains values

$\eta_i(\beta_1, \beta_2, \beta_3)$, $\xi_i(\beta_1, \beta_2, \beta_3)$ – functions of Euler's angles attributed to recalculation of tensor components at coordinate axes turn

θ – turn angle of rod cross-section related with flexural strain

θ' – θ derivative by l coordinates

λ – coordinate referred perpendicularly to l

μ – transversal strain factor

τ – shear stress

ω – turn angle of rod cross-section related to shear strain

References

Beverte I.V. and Kregers A.F. (1987): *Stiffness of lightweight open-porosity foam plastics*. – Mechanics of Composite Materials, vol.23, No.1, pp.27-33.

Brandel B. and Lakes R.S. (2001): *Negative Poisson's ratio polyethylene foams.* – J. Materials Science, vol.36, pp.5885-5893.

Chan N. and Evans K.E. (1997): *Microscopic examination of the microstructure and deformation of conventional and auxetic foams*. – J. Materials Science, vol.32, pp.5725-5736.

Choi J.B. and Lakes R.S. (1995): *Nonlinear analysis of the Poisson's ratio of negative Poisson's ratio foams.* – J. Composite Materials, vol.29, No.1, pp.113-128.

Dement'ev A.G. and Tarakanov O.G. (1970a): *Effect of cellular structure on the mechanical properties of plastic foams.* – Polymer Mechanics, vol.6, No.4, pp.519-525.

Dement'ev A.G. and Tarakanov O.G. (1970b): *Model analysis of the cellular structure of plastic foams of the polyurethane type*. – Polymer Mechanics, vol.6, No.5, pp.744-749.

Gibson L.J. and Ashby M.F. (1982): *The mechanics of three-dimensional cellular materials.* – Proc. Roy. Soc. London, vol.A382, pp.43-59.

Gibson L.J. and Ashby M.F. (1997): *Cellular Solids: Structure and Propertie*s. – Cambridge: Cambridge University Press.

Goldman A.Ya. (1979): *Strength of Constructional Plastics*. – Leningrad: Mashinostroenie (in Russian).

Gromov V.G. and Raetzky G.N. (1971): *Stability and supercritical regime of compressed viscoelastic rod.* – International Applied Mechanics, vol.7, No.12, pp.87-96.

Hilyard N.C. and Cunningham A. (1994): *Low Density Cellular Plastics: Physical Basis of Behaviour.* – London: Chapman and Hall.

Hudson D.G. (1964): *Statistic. Lecture on Elementary Statistics and Probability*. – Geneva: CERN.

Landau L.D., Lifshitz E.M., Kosevich A.M. and Pitaevskii I.P. (1986): *Theory of Elasticity.* – London: Pergamon Press.

Lederman J.M. (1971): *The prediction of the tensile properties of flexible foams.* – J. Appl. Polymer Sci., vol.15, No.3, pp.696-703.

Nyashin M.Y., Osipov A.P., Bolotova M.Ph., Nyashin Y.I., Simanovskaya E.Y. (1999): *Periodontal ligament may be viewed as a porous material filled by free fluid: experimental proof.* – Russian J. Biomechanics, vol.3, No.1, pp.89-95.

Overaker D.W., Lagrana N.A., Cuitiño A.M. (1999): *Finite element analysis of vertebral body mechanics with a nonlinear microstructural model for the trabecular core.* – J. Biomechanical Eng., vol.131, pp.542-550.

Rzhanitsyn A.R. (1968): *Theory of Creep.* – Moscow: Nauka (in Russian).

Shilko S.V., Stelmakh S.V., Chernous D.A. and Pleskatchevskii Yu.M (1998): *Structural simulation of supercompressible materials.* – J. Theor. and Appl. Mechanics, No.1, pp.87-96.

Starovoitov E.I. (2001): *Foundations of the theory of elasticity, plasticity and viscoelasticity*. – Gomel: BelSUT (in Russian).

Wang Y and Cuitiňo A.M (2000): *Three-dimensional nonlinear open-cell foams with large deformations.* – J. Mech. and Phys. Solids, vol.48, No.5, pp.961–988.

Warren W.E. and Kraynik A.M. (1987): *The effective elastic properties of low-density foams.* – The Winter Annual Meeting of the ASME, Boston, December 18-23, pp.123-145.

Weaire D. and Fortes M.A. (1994): *Stress and strain in liquid and solid foams*. – Advances in Physics, vol.43, No.6, pp.685-738.

Received: April 12, 2002
Revised: December 15, 2002